Journal of Membrane Science & Research

journal homepage: www.msrjournal.com

Research Paper

Matrimid® 5218/AO-PIM-1 Blend Membranes for Gas Separation

Mariagiulia Longo [1], Bibiana Comesaña-Gándara [2], Marcello Monteleone [1], Elisa Esposito [1], Alessio Fuoco [1], Lidietta Giorno [1], Neil Bruce McKeown [2], Johannes Carolus Jansen [1,*]

[1] *Institute on Membrane Technology, National Research Council of Italy (CNR-ITM), via P. Bucci 17/C, Rende (CS), 87036, Italy*
[2] *EaStCHEM, School of Chemistry, University of Edinburgh, David Brewster Road, Edinburgh, EH9 3FJ, UK*

Article info

Received 2021-10-07
Revised 2021-11-03
Accepted 2021-11-04
Available online 2021-11-04

Keywords

Polymer blend
Polymer of intrinsic microporosity
Polyimide
Gas separation membrane
Maxwell model

Highlights

- Membranes consisting of blends of AO-PIM-1 and Matrimid® 5218 are prepared
- SEM observations suggest poor compatibility between the two polymers
- Transport properties are dominated by Matrimid® 5218
- Silicone coating successfully heals pinhole defects
- The suitability of the Maxwell model and the model for miscible blends is discussed

Graphical abstract

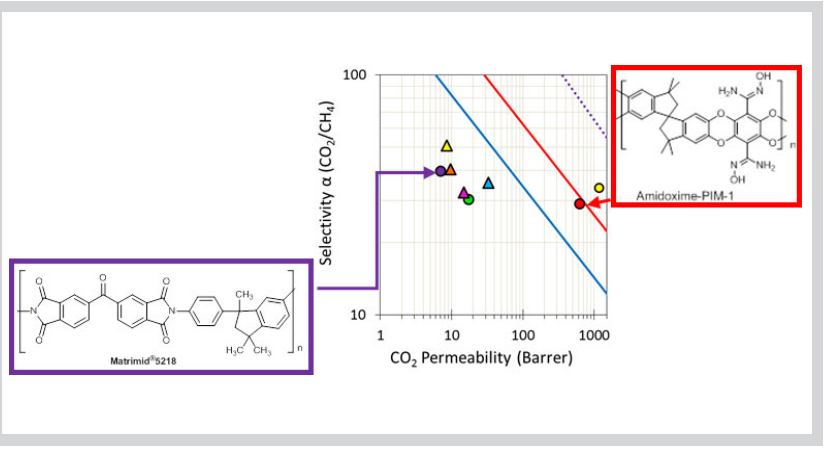

Abstract

In the search for more efficient gas separation membranes, blends offer a compromise between costly high-performance polymers and low-cost commercial polymers. Here, blends of the polymer of intrinsic microporosity, AO-PIM-1, and commercial Matrimid® 5218 polyimide are used to prepare dense films by solution casting. The morphology of the pure polymers and their blends with 20, 40, 60 and 80 wt% of AO-PIM-1 in Matrimid® are studied by scanning electron microscopy (SEM), and their pure gas permeability is studied as a function of the blend composition with H_2, He, O_2, N_2, CH_4 and CO_2. The polymers were found only partially miscible and a two-phase structure was formed with large domains of each polymer. When necessary, the films were coated with a thin silicone layer to heal possible pinhole defects. Even small amounts of Matrimid® in AO-PIM-1 resulted in an unexpectedly strong decrease in the permeability of the PIM, whereas a small amount of the PIM led to a modest increase in permeability of Matrimid®. Due to the two-phase structure, the Maxwell model was more suitable to describe the gas permeability as a function of the blend composition than the model for miscible blends. At low Matrimid® concentrations in AO-PIM-1, all models fail to describe the experimental data due to an unexpectedly strong depression of the permeability of the PIM by Matrimid®. Time lag measurements reveal that the changes in permeability as a function of the blend composition are mostly due to changes in the diffusion coefficient.

1. Introduction

The development of membrane technology plays an important role in several large-scale and emerging gas separation applications [1], also under harsh conditions [2]. Generally, commercial glassy polymers used for gas separation membranes, such as polysulfones, polyethersulfones and polyimides have a good selectivity (purity of the products), but low permeability (productivity) [3]. Most high-performing polymers with a combination of high permeability and good selectivity, such as thermally rearranged (TR) polymers [4,5] and polymers of intrinsic microporosity (PIMs) [6,7] are expensive and the synthesis is difficult to realise at industrial scale, or have other issues such as physical aging [8]. A possible way to boost the use of expensive high-performance polymers in large-scale applications is by blending them with a second inexpensive polymer. Potentially, this strategy combines the advantages of each polymer into a blended product and obtains the desired properties that differ from those of the individual polymers [9]. The ability to predict the gas permeability coefficients in blends from the gas permeability coefficients in the two neat polymers could help the identification of the most promising blend materials for membrane preparation. A simple equation for predicting the permeability of a homogeneous miscible blend was proposed by Robeson [10], and the gas permeability in the blend, Pb, is empirically correlated with the gas permeabilities and the volume fractions of the neat components:

$$\ln P_b = \varphi_1 \ln P_1 + \varphi_2 \ln P_2 \quad (1)$$

* Corresponding author: johannescarolus.jansen@cnr.it (J.C. Jansen)

DOI: 10.22079/JMSR.2021.540493.1504

where φ_1 and φ_2 are the volume fractions of the two polymers in the blend, and P_1 and P_2 are their respective permeabilities [10]. One of the possible problems of polymer blends is the limited miscibility and homogeneity of the blend components. Miscible blends are homogeneous systems where the two or more materials dissolve in each other at the molecular level, exhibiting single phase properties. Instead, in immiscible blends, the two components do not completely dissolve in each other, thus resulting in the formation of two different phases. For systems where the dispersed phase is less than ca. 30 vol% and consists of spherical particles, the Maxwell model is one of the simplest and most commonly employed models to describe the gas transport [11–14]:

$$P_{MMM} = P_c \left[\frac{P_d + 2P_c - 2\varphi_d(P_c - P_d)}{P_d + 2P_c + \varphi_d(P_c - P_d)} \right] \quad (2)$$

where the P_{MMM} is the effective permeability of the mixed matrix membrane, P_c and P_d are the gas permeabilities in the continuous and dispersed phase, respectively, and φ_d is the volume fraction of the dispersed phase. The gas transport in a mixed matrix membrane depends on the two different phases and on the nature of their interface, and several fundamentally different cases were discussed by Koros *et al.* [15].

A widely studied polymer for gas separation membranes is Matrimid® 5218 due to its good selectivity and processability. However, its relatively low gas permeability is insufficient for large-scale applications, such as CO_2 capture from flue. A possible route to overcome this limitation is the blending with a Polymer of Intrinsic Microporosity (PIM) to exploit the high selectivity of Matrimid® and the exceptionally high permeability of the PIM [16]. Blends of Matrimid® 5218 with PIM-1 were first reported by Yong *et al.* [17], who enhanced the O_2/N_2 permselectivity by adding little Matrimid® 5218 to PIM-1 and the CO_2/CH_4 gas separation performance by adding little PIM-1 to an excess of Matrimid® 5218. With their PIM-1/Matrimid® 5218 blend hollow fibres, they obtained an ultrathin dense layer and membranes of potential industrial interest [18], drastically reducing the amount of PIM-1 with respect to pure PIM-1 fibres [19]. More recently, the comparison between the highly selective Matrimid® 5218, the highly permeable PIM-EA(H_2)-TB and their 50/50 wt% blend membrane showed an increase of permeability of Matrimid® 5218 by the addition of the ethanoanthracene-based PIM, whilst maintaining a reasonably high selectivity [20].

The present work discusses the preparation and characterization of blends of amidoxime-functionalized PIM-1 (AO-PIM-1) and the commercial polyimide Matrimid® 5218 (Figure 1). The incorporation of a high free volume PIM, such as AO-PIM-1, into Matrimid® is expected to give an overall increase in the fractional free volume (FFV) [17]. The principal aim is to enhance the permeability of Matrimid® 5218 by the addition of AO-PIM-1, and to find the optimum combination of the high permeability of the PIM and the high selectivity of the polyimide. We further aim to increase our understanding of the degree of interaction of the two polymers, of their mutual miscibility, and in particular of the effect of the blend composition and morphology/microstructure on the transport properties. The use of the AO-PIM-1 rather than other PIMs is inspired by a previous study in which Swaidan *et al.* show how the AO-modification induced a tightening of the polymeric matrix and an improvement of the selectivity over PIM-1 [21]. The analysis of single gas permeability, solubility and diffusivity will provide detailed insight into the effect of the blend composition on the overall transport properties of the novel blends. The properties will be described by common models for homogeneous blends or for mixed matrix systems, in order to correlate the permeability with the membrane composition and microstructure.

2. Materials and methods

2.1. Materials

Matrimid® 5218 was kindly supplied by Huntsman (Basel, Switzerland). PIM-1 (average molar mass of around 200 kg mol^{-1} relative to polystyrene standards) was synthesized according to the procedure reported by Budd *et al.* [22]. A mixture of 5,5',6,6'-tetrahydroxy-3,3,3',3'-tetramethyl-1,1'-spirobisindane (TTFPN), 2,3,5,6-tetrafluoroterephthalonitrile and anhydrous N,N-dimethylformamide (DMF 99.8%) was stirred under a dry nitrogen atmosphere and heated at 65 °C for 3 days. After cooling down to room temperature, the reaction mixture was slowly poured into water and the precipitate was collected by filtration. The AO- modification was achieved by dissolving PIM-1 in tetrahydrofuran (THF 99.9%) and reacting it with excess hydroxylamine at 65 °C according to the method reported by Patel *et al.* [23]. Two-component polydimethylsiloxane (PDMS) resin ELASTOSIL® M 4601, consisting of a pre-polymer A and crosslinker B, was purchased from Wacker Chemie AG.

2.2. Preparation of Matrimid® 5218/AO-PIM-1 blend membranes

AO-PIM-1/Matrimid® dense films were prepared by the solution casting and solvent evaporation method, using anhydrous dimethylacetamide, DMAc, as the solvent. The pure Matrimid® solution was prepared at a concentration of 3 wt%, and a homogenous solution was obtained under magnetic stirring overnight. The pure AO-PIM-1 solutions were prepared at concentrations between 2% and 3%. Blend solutions were obtained by mixing a fixed amount of the Matrimid® 5218 solution (containing 0.140 g of Matrimid®) with different amounts of AO-PIM-1 solution to yield mixtures with 20, 40, 60 and 80 wt% of AO-PIM-1 in Matrimid® 5218 after solvent evaporation. The resulting solutions were stirred until they became homogeneous and were then filtered (3.1 µm GMF syringe filters) to remove possible dust or polymer gel particles. Membranes were casted by pouring the solutions into a glass Petri dish of 12 cm in diameter, which were then placed in an oven at 50 °C for at least 5 days. The dense films were labelled as Matrimid®_AO-PIM-1 xx_yy, where xx_yy represent the weight percentages of the two polymers, as reported in Table 1. The thickness of the membranes was measured with a Mitutoyo model IP65 digital micrometer as an average of at least 8 individual measurements on different areas of the same sample.

Table 1
Membrane codes and percentage of AO-PIM-1 in the final membrane.

Name: Matrimid® 5218_AO-PIM-1	Matrimid® (mg)	AO-PIM-1 (mg)	AO-PIM-1 content (wt%)	Membrane thickness (µm)[a]
100_0	140	0	0	19.1 ± 3.5
80_20	140	35	20	11.2 ± 3.4
60_40	140	93	40	30.2 ± 6.5
40_60	140	210	60	54.8 ± 7.5
20_80	140	560	80	74.8 ± 12.3
0_100	0	455	100	39.0 ± 4.9

[a] Average thickness and standard deviation from at least 8 individual measurements on the same membrane without silicon coating.

2.2.1. Coating of the membranes with PDMS

A solution of PDMS ELASTOSIL® M 4601 was applied on membranes that showed unreasonable permeability values in order to heal occasional pinhole defects. The two components of PDMS were mixed in the weight ratio 9:1 according to the instructions of the supplier and dissolved in cyclohexane in order to obtain a solution of 80 wt% cyclohexane, 18 wt% of base polymer (component A) and 2 wt% of curing agent (component B). The solution was stirred for 1 hour at 60°C to promote a partial polymerization [24]. After cooling, the solution was further diluted with cyclohexane to obtain a final concentration of 10 wt% silicone resin. The coating was applied manually with a pipette, while slightly tilting the membranes to allow the excess solution to flow away. The membranes were left to dry for several days at room temperature, allowing the total evaporation of the solvent and the crosslinking of the polymer. The final thickness of the coating layer was approximately 5 µm.

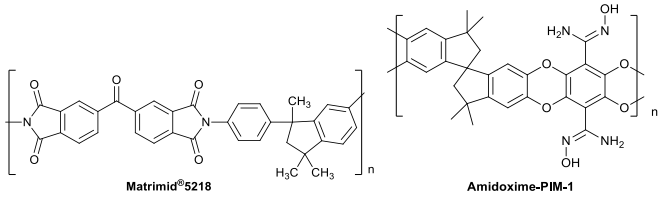

Fig. 1. Chemical structures of Matrimid® 5218 and AO-PIM-1

2.3. Membranes characterization

Morphological and chemical analysis of membranes were performed by scanning electron microscopy (SEM) on a Phenom Pro X desktop SEM (Phenom-World B.V., Eindhoven, The Netherlands), equipped with backscattering detector (BSD), and by infrared spectroscopy (FT-IR) analysis

on a Spectrum Spotlight Chemical Imaging Instrument (PerkinElmer) with universal ATR sampling accessory. Before SEM analysis, all samples were sputter-coated with a thin layer of gold to minimise the charge and improve the image quality. Single gas permeation tests were carried out at 25 °C and at a feed pressure of 1 bar, using a fixed-volume pressure increase instrument (designed by HZG and constructed by ESSR, Geesthacht, Germany). The permeability, *P*, and diffusivity, *D*, were determined by the well-known time-lag method [25]. The ideal selectivity is the ratio of the permeability of two species, $\alpha_{(A/B)} = P_A/P_B$. The so-called solution-diffusion model for gas transport in dense membranes describes the permeability as the product of the solubility coefficient, *S*, and the diffusion coefficient. The solubility was therefore calculated indirectly as $S=P/D$.

3. Results and discussion

3.1. Membrane morphology

All membranes showed high optical transparency, suggesting the formation of a homogeneous phase and good compatibility of the two polymers. However, while the SEM images of the top surface of the neat polymer membranes appear dense and uniform (Figure 2), micro phase separation and domains of different size and shapes are visible in the blend surface.

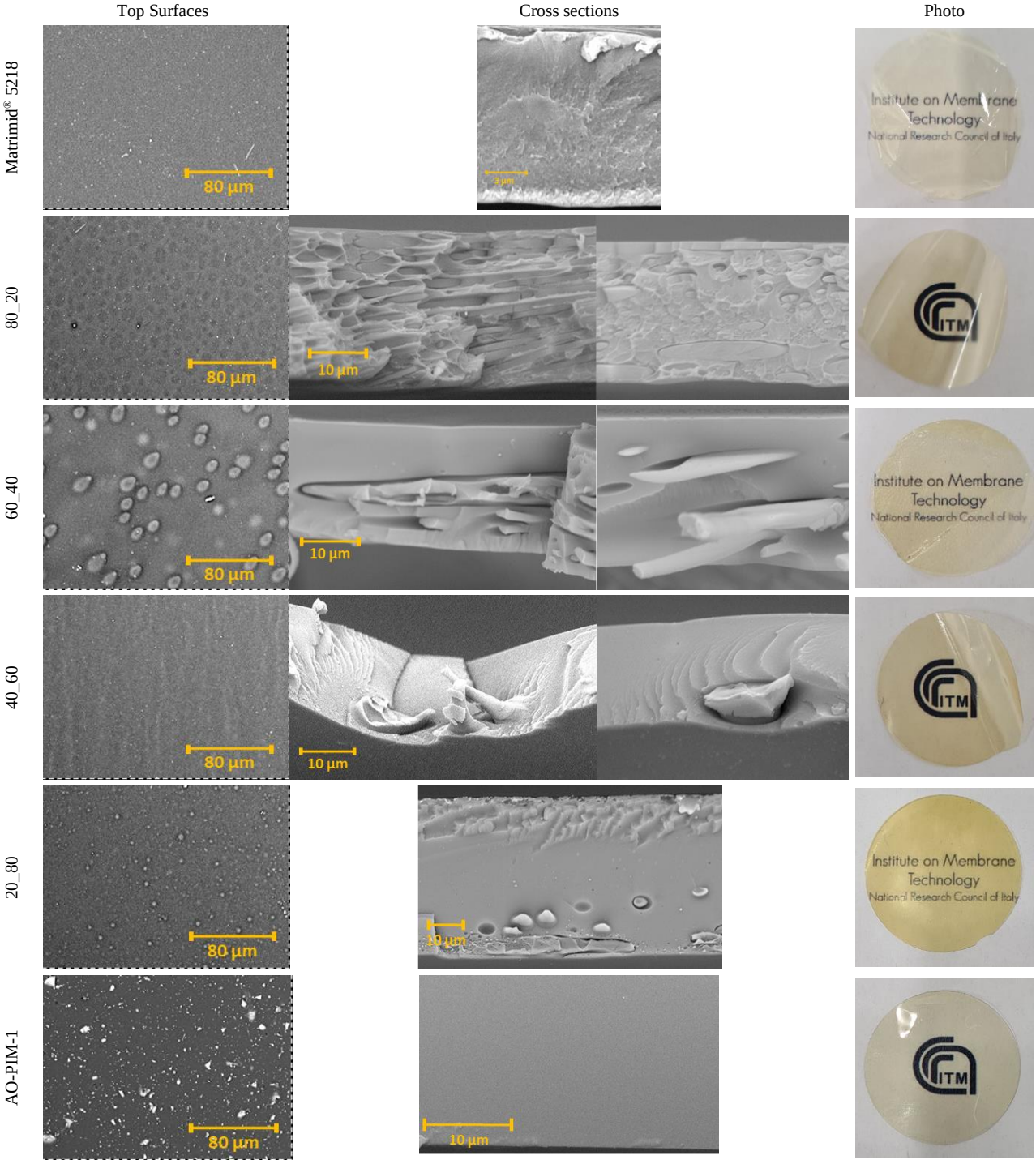

Fig. 2. SEM images of the surface and cross sections of the pure Matrimid®5218 and AO-PIM-1 membranes, and their blends with compositions of 20, 40, 60 and 80 wt% of AO-PIM-1. Photographs of 2.5 cm circular membranes demonstrate their optical transparency.

The cross section of the membrane with 20 wt% of AO-PIM-1 shows a layered structure, in which AO-PIM-1 domains of different shape are clearly distinct from the Matrimid® 5218 bulk. Qualitatively, the volume fraction of the dispersed phase in this sample seems to be higher than 20 % of the total volume. This suggests a partial solubility of Matrimid® 5218 in the phase-separated AO-PIM-1. Phase separation is clearly observed in the cross sections of all other blends as well, and the domains of the two polymers have different shapes and dimensions. Thus, the two polymers are poorly compatible and the optical transparency must be a result of the apparently very similar refractive indices of the two polymers. The relatively large domains of the phase separated polymers are a result of the slow evaporation of the solvent and the long-time available for the nucleation and growth of the domains of the phase separated polymers.

The IR-spectra of the neat polymers and their blends are shown in Figure 3a, and provide information on the chemical interaction between Matrimid® 5218 and AO-PIM-1. The spectrum of Matrimid® 5218 exhibits the characteristic bands of polyimides, denoted by asymmetric and symmetric C=O stretching vibration bands around 1780 and 1720 cm^{-1}; asymmetric C-N stretching at 1365 cm^{-1}; stretching of C-N-C groups at 1102 cm^{-1}; and the out-of-plane bending of C-N-C groups around 725 cm^{-1}.

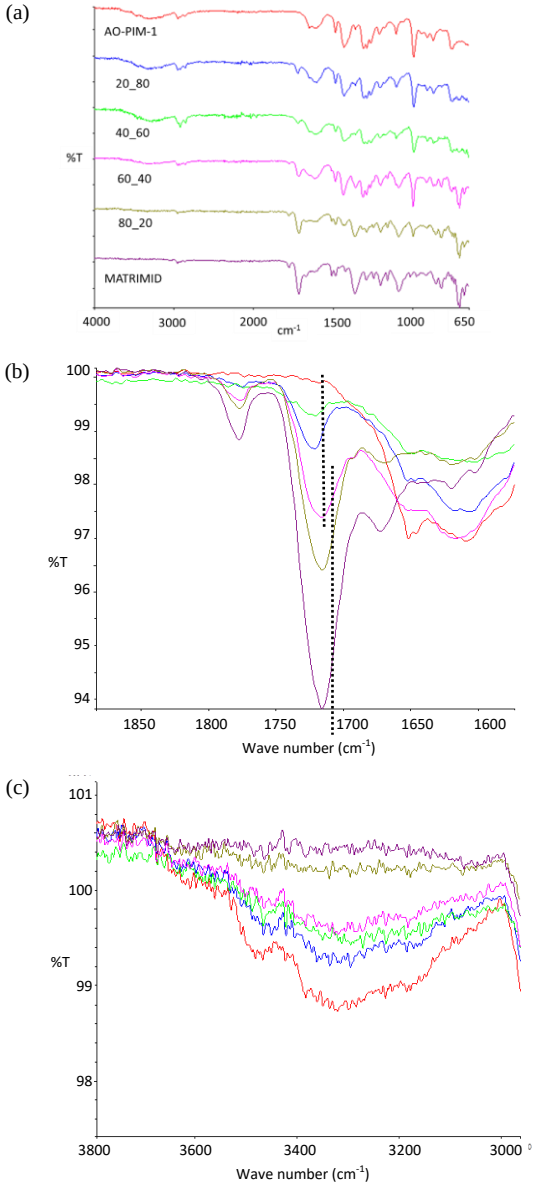

Fig. 3. (a) ATR-FTIR spectra of the Matrimid® 5218/AO-PIM-1 blends and neat polymer membranes and a zoom of (b) the carbonyl stretching vibration of the Matrimid® 5218 around and (c) the symmetric and asymmetric -NH_2 and -OH stretching vibrations.

The C=O peak is absent in AO-PIM-1 and its intensity gradually increases with increasing Matrimid® 5218 content, with some deviations from the trend that may be due to the heterogeneous nature of the blend (Figure 3b) and the limited sampling depth in ATR mode. Interestingly, the C=O peak shifts to slightly higher wave numbers at the highest AO-PIM-1 content, where Matrimid® is the dispersed phase. This suggests that interaction between the two polymers occurs, probably by hydrogen bonding between the C=O group of Matrimid® and the -OH and -NH_2 groups of AO-PIM-1, and it supports the hypothesis that Matrimid® is partially soluble in AO-PIM-1. The sharp band at 914 cm^{-1}, ascribed to the N-O stretching vibration mode, representative of the oxime groups, appear in pure AO-PIM-1 and all the blends, but not in pure Matrimid®. The signal at 914 cm^{-1} tends to become more intense with increasing AO-PIM-1 content, and also in this case some deviations from the trend (*e.g.* remarkably strong signal at 40 wt% AO-PIM-1) may be due to the sample heterogeneity. An increasingly intense broad band emerges in the region of 3600 – 3100 cm^{-1}, (Figure 3c), involving overlapping bands that are assigned to the asymmetric and symmetric stretching mode of -NH_2 groups (3480 and 3340 cm^{-1}, respectively) and the stretching vibration mode of the -OH groups (3175 cm^{-1}), both characteristic of AO-PIM-1.

3.2. Pure gas transport properties

Single gas permeation measurements of the pure polymers Matrimid® 5218 and AO-PIM-1 and the blend membranes were carried out in the order H_2, He, O_2, N_2, CH_4 and CO_2. For those samples with pinholes, the membranes were coated with PDMS, which is the standard procedure used also in commercial membranes to heal defects and increase their separation performance [26–28]. In the presence of the PDMS coating layer, the resistance of the membrane to gas permeation can be expressed as the sum of the contributions of the pristine membrane and the PDMS coating layer (resistances-in-series model) [29]. Considering that the gas permeability in PDMS is orders of magnitude higher than that of the blends, and considering the thickness of the PDMS layer of about 5 µm, much lower than that of the blend, the effect of PDMS on the overall transport resistance is negligible. Thus, its only effect is the elimination of the Knudsen diffusion through the pinholes in the membrane, as visible from the flat baseline in the initial stage of the curve of the coated membrane, whereas the permeate pressure in the uncoated membrane increases instantaneously after exposure to the gas (Figure 4).

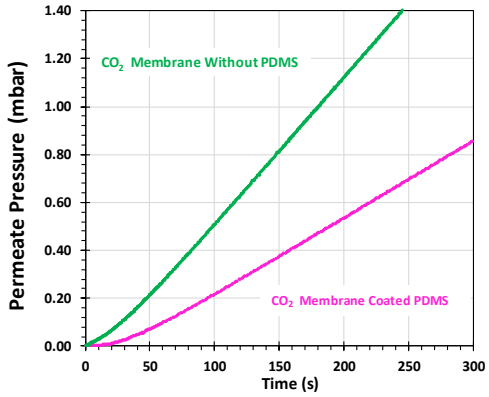

Fig. 4. Example of CO_2 pure gas permeation curves of membrane Matrimid_AO-PIM1_80_20 with and without PDMS coating.

Since the permeability and the diffusion coefficient of the blends were expected to increase with increasing AO-PIM-1 content, the same amount of Matrimid® was used for each membrane and the appropriate amount of AO-PIM-1 was added to this solution. The final thickness of the membranes increases with increasing PIM content, avoiding extreme differences in the time lag and allowing a direct comparison of the data (Table 1). The results of the measurements are summarised in Table 2, reporting only the data of the PDMS-coated film in case healing of pinholes was necessary. For a qualitatively better understanding, Figure 5 shows the trends of the gas transport parameters of the membranes as a function of the AO-PIM-1 concentration in the membrane. The results highlight quite different properties of Matrimid® 5218 and the blends on the one hand, and pure AO-PIM-1 on the other hand.

Table 2
Effective permeability, diffusion and solubility coefficients, and their respective selectivity values of Matrimid® 5218/AO-PIM-1 blend membranes, tested at 25°C and 1 bar of feed pressure. Samples are measured as cast or after PDMS coating in the case of pinhole defects.

Matrimid® 5218_AO-PIM-1	Permeability coefficient (Barrer)						α_P (P_a/P_{N2}) (-)				
(wt%_wt%)	N_2	O_2	CO_2	CH_4	H_2	He	O_2	CO_2	CH_4	H_2	He
100_00 [20]	0.20	1.6	8.6	0.2	22.8	22	8.5	45.3	0.9	120	115
100_00	0.19	1.13	7.0	0.18	13.5	13.4	6.0	37.1	0.93	71.9	71.1
80_20*	0.26	1.6	9.7	0.24	19.9	19.4	6.2	37.1	0.92	76.1	74.1
60_40	0.43	2.0	15.0	0.46	19.1	16.7	4.7	34.4	1.1	44.2	38.7
40_60	0.42	2.3	17.2	0.57	20.3	17.7	5.4	41.4	1.4	48.6	42.5
20_80*/**	0.79	4.2	33.0	0.92	37.0	29.0	5.3	41.7	1.2	47	36.9
00_100	18	75.0	625	21.5	417	218	4.2	34.7	1.2	23.2	12.1
00_100 [21] ***	33	147	1153	34	912	412	4.5	35	1.0	27.6	12.5
	Time lag (s)										
	N_2	O_2	CO_2	CH_4	H_2	He					
100_000_	130	30.3	130	686	0.37	0.25					
80_20*	31.3	7.50	33.9	180	0.09	0.02					
60_40	167	627	168	742	0.63	0.25					
40_60	393	113	387	1438	2.60	0.37					
20_80*/**	999	260	750	3747	4.92	1.42					
00_100	47.5	12.2	29.2	192	0.33	0.11					
	Diffusion coefficient (10^{-12} m^2 s^{-1})						α_D (D_a/D_{N2}) (-)				
	N_2	O_2	CO_2	CH_4	H_2	He	O_2	CO_2	CH_4	H_2	He
100_000 [20]	0.2	1.2	0.3	0.10	/	/	5.7	1.3	0.20	/	/
100_000_	0.51	2.1	0.47	0.10	/	/	4.1	0.92	0.18	/	/
80_20*	0.65	2.9	0.60	0.11	208	849	4.4	0.93	0.17	318	1300
60_40	0.88	2.9	0.90	0.20	243	612	3.3	1.0	0.23	275	670
40_60	1.2	4.2	1.3	0.35	193	1365	3.5	1.0	0.29	160	1139
20_80*/**	0.93	3.6	1.2	0.25	190	659	3.8	1.3	0.27	203	705
00_100	5.4	20.5	8.7	1.3	775	2381	3.9	1.6	0.25	134	116
00_100 [21] ***	9.9	40.6	24.6	2.6	/	/	4.1	2.5	0.26	/	/
	Solubility coefficient (cm^3_{STP} cm^{-3} bar^{-1})						α_S (S_a/S_{N2}) (-)				
	N_2	O_2	CO_2	CH_4	H_2	He	O_2	CO_2	CH_4	H_2	He
100_000 [20]	0.7	1	23	3.5	/	/					
100_000_	0.28	0.41	11.2	1.5	/	/	1.5	40.0	5.3	/	/
80_20*	0.30	0.42	12.1	1.6	0.07	0.02	1.4	40.0	5.3	0.24	0.06
60_40	0.37	0.53	12.3	1.7	0.06	0.02	1.4	33.5	4.6	0.16	0.06
40_60	0.26	0.40	10.0	1.2	0.08	0.01	1.5	38.3	4.7	0.30	0.04
20_80*/**	0.63	0.88	19.8	2.8	0.15	0.03	1.4	31.3	4.4	0.23	0.05
00_100	2.5	2.7	54.0	12.2	0.44	0.26	1.1	21.4	4.9	0.17	0.10
00_100 [21] ***	2.7	2.7	34.4	10.0	/	/	1.0	12.7	3.7	/	/

1 Barrer = 10^{-10} cm^3 (STP) cm cm^{-2} $cmHg^{-1}$ s^{-1}
**Sample after PDMS coating, **Aged 7 months, ***Test and preparation conditions: T=35 °C, 2 bar; 24 h methanol soak; dried under vacuum at 120 °C for 24 h.

For all gases, the permeability, the diffusivity and the solubility gradually increase with the increasing PIM content (Figure 5a, 5c and 5e). The permeability of pure AO-PIM-1 is much higher with respect to Matrimid® and all blends, leading to a strong discontinuity. The permselectivity is generally lower in AO-PIM-1, especially for gas pairs with very different kinetic diameters, like H_2/N_2 and He/N_2, Figure 5b. This is due to the different transport mechanism of H_2 and He in PIMs [30], which sense the free volume differently due to the higher interconnectivity of the free volume for these gases. The higher free volume in AO-PIM-1 [21] in the blends causes an increase of the diffusion coefficient with increasing PIM content in the blend series, Figure 5c. For gases with large size, e.g. CH_4 and CO_2, the diffusion selectivity with respect to N_2 increases with AO-PIM-1 content, while it is mostly constant for O_2/N_2, Figure 5d. The solubility increases linearly with the amount of AO-PIM-1 in the blend, Figure 5e. The solubility selectivity is almost constant for all gas pairs Figure 5f. The trends in the effect of the blend composition on the gas permeability are best seen in the Robeson diagrams for CO_2/N_2, CO_2/CH_4, O_2/N_2 and H_2/N_2 (Figure 6). Literature data of pure Matrimid® and AO-PIM-1 are also plotted for reference. The general trends in the diagrams show an increase in the pure gas permeability with increasing AO-PIM-1 content, accompanied by a modest decrease in ideal selectivity compared to the neat Matrimid® membrane.

The CO_2/CH_4 selectivity of the blends is similar to that of neat Matrimid® 5218, while the CO_2 permeability increases only slightly (Figure 6a). The higher CO_2/N_2 selectivity in Matrimid®_AO-PIM-1_20_80, Figure 6b, must be ascribed mainly to the higher solubility selectivity, Figure 5f. The O_2/N_2 selectivity, Figure 6c, is higher in Matrimid® 5218 due to a slightly higher solubility selectivity, whereas the diffusivity selectivity, Figure 5d, is roughly the same for both neat polymers and the set of blends. In general, the selectivity is higher in Matrimid® 5218, especially for gas pairs with very different kinetic diameters, like H_2/N_2, Figure 6d, mainly as a result of the higher diffusion selectivity. The discontinuity in the permeability between the blends and the neat AO-PIM-1 suggests that even small amounts of Matrimid® apparently occupy a part of the original free volume of the AO-PIM-1, thus reducing drastically the permeability of the neat PIM. The FT-IR analysis above confirmed the interaction between the two polymers and showed that at low Matrimid® content, the carbonyl groups of the polyimide interact with the AO-PIM-1 matrix, resulting in a shift to slightly higher wave numbers.

Figure 7 shows the trends predicted by Eq. 1 and Eq. 2. The limited miscibility of the two blend components is the main reason for the deviations of permeability from the logarithmic trend predicted by Eq. 1, which is unsuitable in this case. Indeed, a more appropriate model for immiscible blends is the Maxwell model (Eq. 2). The Maxwell model was used because of its simplicity and the absence of adjustable parameters, although more sophisticated models may be more suitable that account for the non-uniform size and shape of the dispersed phase [31].

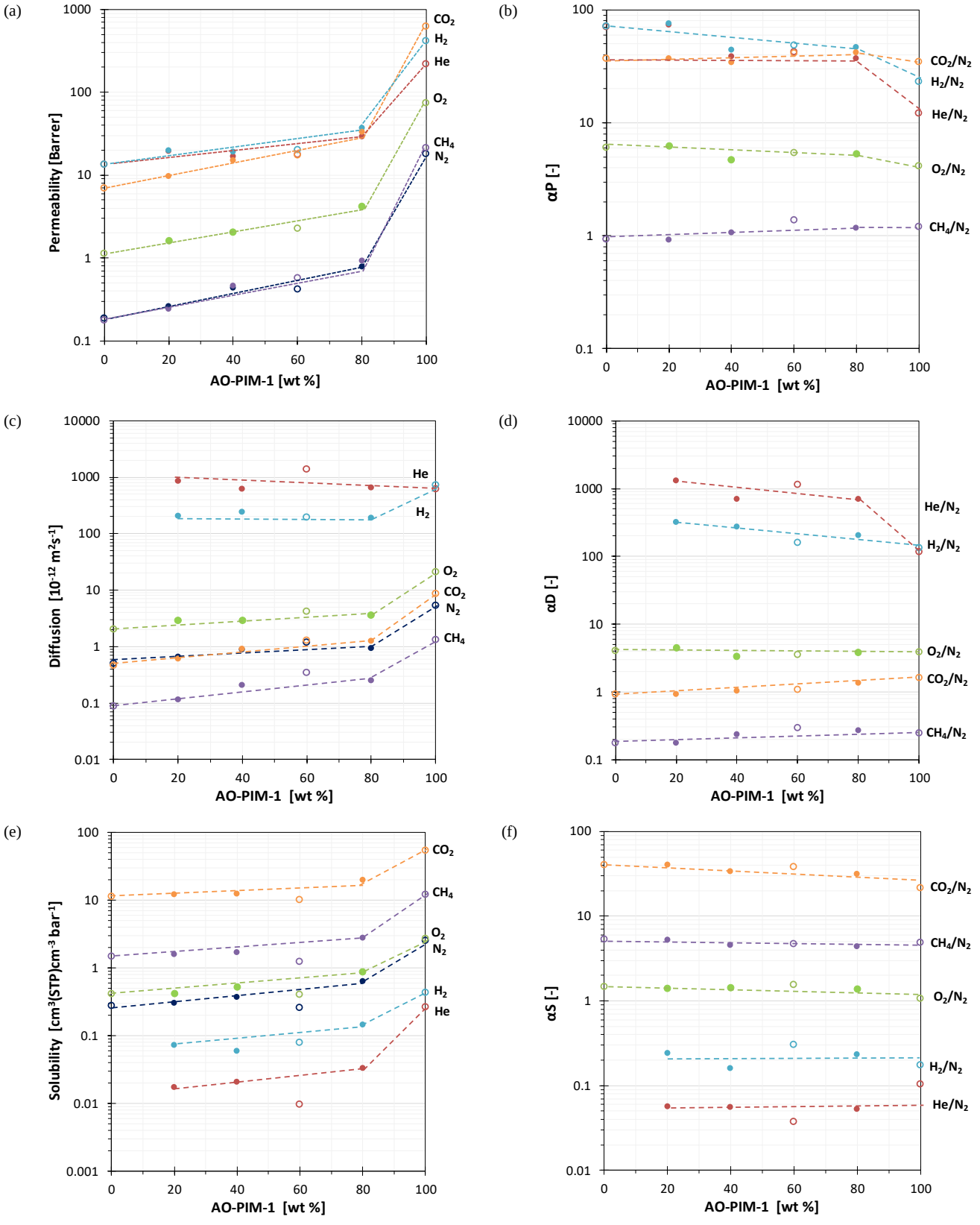

Fig. 5. Permeability, diffusivity, solubility (a,c,e) and their respectively selectivity (b,d,f) of six gasses as a function of the AO-PIM-1 content in Matrimid® 5218/AO-PIM-1 blend membranes. Open symbols indicate the as-cast membranes and filled symbols indicate the membranes coated with PDMS, in case defect healing was necessary. The data of the membrane with 20% AO-PIM-1 refer to a sample aged for 7 months. The lines only serve as a guide to the eye.

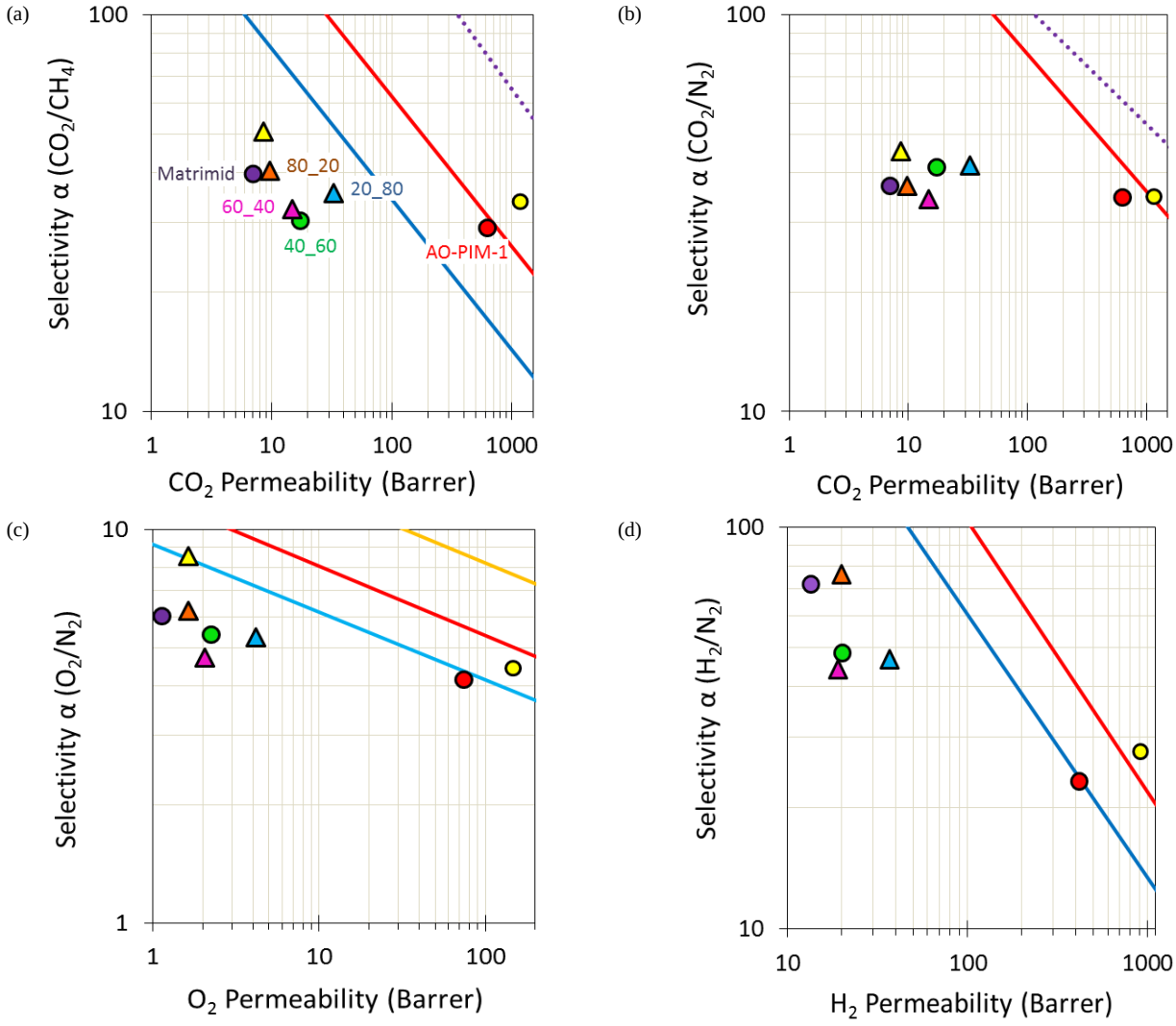

Fig. 6. Robeson plots of membranes: ● pure AO-PIM-1, ● pure Matrimid®, ▲ Matrimid®_AO-PIM-1_20_80_PDMS_aged 7 months, ● Matrimid®_AO-PIM-1_40_60, ▲ Matrimid®_AO-PIM-1_80_20_PDMS, ▲ Matrimid®_AO-PIM-1_60_40 for CO_2/CH_4 (a), CO_2/N_2 (b), O_2/N_2 (c) and H_2/N_2 (d) with the 1991 upper bounds indicated by a blue line, 2008 by a red line, 2015 by a yellow line, and 2019 by purple dotted line. Reference data for △ Matrimid® [20] and ○ AO-PIM-1 membranes [21] are plotted for comparison. The AO-PIM-1 reference sample was MeOH treated and had therefore a higher permeability.

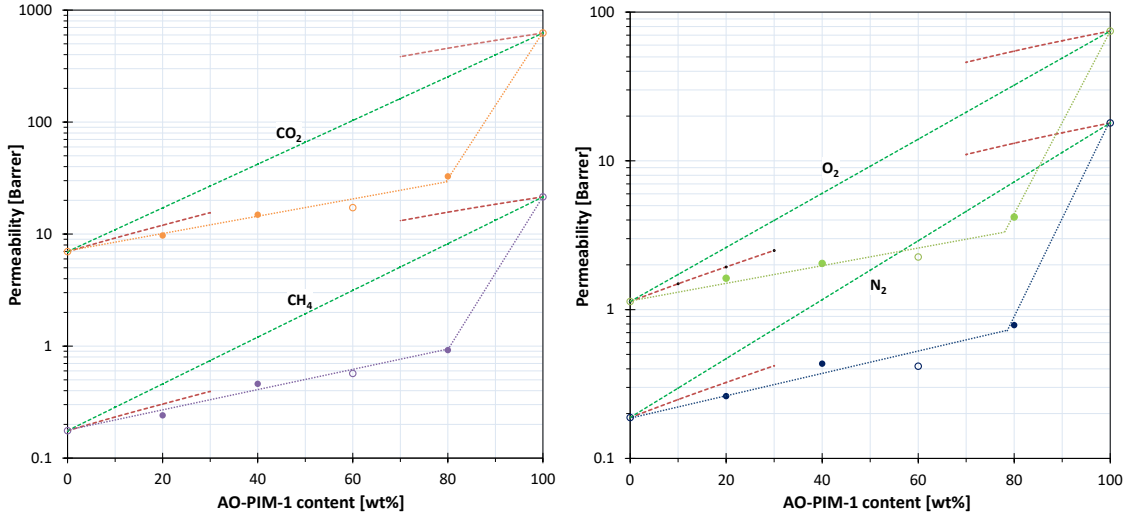

Fig. 7. Experimental permeability of CO_2, CH_4, O_2 and N_2 as a function of the Matrimid®/AO-PIM-1 blend composition, and comparison with the logarithmic model for miscible blends (Eq. 1, green dashed line) and the Maxwell model (Eq. 2, red dashed lines, indicated within the limits of its validity). Open symbols

indicate the as cast membranes and filled symbols indicate the membranes coated with PDMS, in case healing was needed.

Although other models may be suitable for higher loadings or non-spherical dispersed phases [32], the simple Maxwell model describes the transport properties quite satisfactorily at low AO-PIM-1 concentration in the blend, up to ca. 40 wt%, as shown for CO_2, CH_4, O_2 and N_2 in Figure 7. We may assume that AO-PIM-1 is the dispersed phase in this range, and the Maxwell model fits the experimental data best for CH_4, while it slightly overestimates the data for CO_2, O_2 and N_2. On the other hand, the presence of low amounts of Matrimid® in AO-PIM-1 dramatically reduces the permeability of the PIM, suggesting that the first and most important effect of Matrimid® is to occupy the free volume of the PIM. Therefore, the trend deviates completely from the Maxwell model for PIM percentages higher than 60%, where Matrimid® is assumed to be dispersed or dissolved in AO-PIM-1. The phase behaviour could be confirmed by analysis of the additive (or non-additive) behaviour of the density, but the reported densities of Matrimid® and AO-PIM-1 reported, 1.24 g cm^{-3} [33] and 1.18 g cm^{-3} [34], respectively, are too similar in this case. Therefore, it is not possible to verify the phase behaviour of the two polymers accurately with the help of their density. The permeability appears to be much more sensitive, and decisive in combination with SEM analysis.

To some extent, the deviation from the trend might also be due to slight differences in the degree of physical aging in the samples, typically observed for PIMs but to a lesser extent in common glassy polymers with lower free volume. This could not be investigated systematically with the present blends, because the commonly used alcohol treatment to reset the casting history, damaged the films because of their heterogeneous nature and the different degrees of swelling of the two phases. In any case, aging is much slower in as-cast membranes [35] and therefore we believe that this effect is of minor importance.

4. Conclusions and future perspectives

The performance of the heterogeneous Matrimid® 5218/AO-PIM-1 blends was evaluated in terms of their pure gas permeation properties. The newly developed blend membranes show intermediate gas transport properties between those of Matrimid® 5218 and AO-PIM-1, with diffusivity coefficients that increase with increasing PIM content in the blend. This is ascribed to the presumed increase of free volume by the presence of AO-PIM-1 in the Matrimid® and is further supported by the trends in solubility and permeability. The permeability at low PIM contents (< 40%) is described fairly well by the Maxwell model for CH_4, while the experimental values are somewhat lower than the model for CO_2, O_2 and N_2. At higher AO-PIM-1 content, assuming Matrimid® as the dispersed phase, the experimental permeability is much lower than the predictions by the Maxwell model and even lower than the predictions by the miscible blend model, which are both inadequate. In all cases, blend membranes exhibit a higher permselectivity than pure AO-PIM-1. The best performing blend membrane is the one with the smallest amount of PIM (Matrimid® 5218_AO-PIM-1_80_20). For this membrane the permeability increases substantially, whereas the permselectivity remains the same as in Matrimid® 5218. Therefore, the AO-PIM-1 offers the possibility to increase the permeability of Matrimid® 5218, maintaining a reasonably high selectivity. The unexpectedly low permeability of AO-PIM-1 with a low amount of Matrimid® may be related to specific interactions of the functional groups in Matrimid® and the polar AO group in the PIM. The relatively strong decrease in the diffusion coefficient is apparently due to a significant loss of the intrinsic microporosity and free volume.

Comparison of the two models defined by Eq. 1 and Eq. 2 show that in immiscible blends, following the Maxwell model, small amounts of the PIM improve the permeability of the low-permeable polymer bulk much less than in miscible blends. More effort is therefore needed to find a compatible polymer for AO-PIM-1. Since large domains were formed upon slow evaporation of the solvent, this suggests that the morphology may be finer in the case of a higher evaporation rate, for instance when preparing thin film composite membranes. This may be a topic for further studies in order to evaluate whether a fine microstructure could improve the transport properties.

Acknowledgements

Part of the work carried out for this manuscript received financial support from the Fondazione CARIPLO, programme “Economia Circolare: ricerca per un futuro sostenibile” 2019, Project code: 2019-2090, MOCA - Metal Organic frameworks and organic CAges for highly selective gas separation membranes and heavy metal capture devices. J.C.J. acknowledges funding from the CNR Program Short Term Mobility 2019. M. Longo wishes to acknowledge CNR-ITM for the financial support for the PhD mobility period to the University of Edinburgh. Phenom-World B.V., Eindhoven (NL), is gratefully acknowledged for providing a Phenom Pro X desktop SEM for evaluation.

References

[1] E. Esposito, L. Dellamuzia, U. Moretti, A. Fuoco, L. Giorno, J.C. Jansen, Simultaneous production of biomethane and food grade CO2 from biogas: an industrial case study, Energy Environ. Sci. 12 (2019) 281–289. doi:10.1039/C8EE02897D.

[2] J. Deng, Z. Huang, B.J. Sundell, D.J. Harrigan, S.A. Sharber, K. Zhang, R. Guo, M. Galizia, State of the art and prospects of chemically and thermally aggressive membrane gas separations: Insights from polymer science, Polymer (Guildf). (2021) 123988. doi:10.1016/j.polymer.2021.123988.

[3] H.B. Park, J. Kamcev, L.M. Robeson, M. Elimelech, B.D. Freeman, Maximizing the right stuff: The trade-off between membrane permeability and selectivity, Science 356 (2017) eaab0530. doi:10.1126/science.aab0530.

[4] M. Calle, Y.M. Lee, Thermally Rearranged (TR) Poly(ether−benzoxazole) Membranes for Gas Separation, Macromolecules. 44 (2011) 1156–1165. doi:10.1021/ma102878z.

[5] H.B. Park, S.H. Han, C.H. Jung, Y.M. Lee, A.J. Hill, Thermally rearranged (TR) polymer membranes for CO2 separation, J. Memb. Sci. 359 (2010) 11–24. doi:10.1016/j.memsci.2009.09.037.

[6] N.B. McKeown, Polymers of Intrinsic Microporosity (PIMs), Polymer (Guildf). 202 (2020) 122736. doi:10.1016/j.polymer.2020.122736.

[7] S. Bandehali, A. Ebadi Amooghin, H. Sanaeepur, R. Ahmadi, A. Fuoco, J.C. Jansen, S. Shirazian, Polymers of intrinsic microporosity and thermally rearranged polymer membranes for highly efficient gas separation, Sep. Purif. Technol. 278 (2022) 119513. doi:10.1016/j.seppur.2021.119513.

[8] Z.-X. Low, P.M. Budd, N.B. McKeown, D.A. Patterson, Gas Permeation Properties, Physical Aging, and Its Mitigation in High Free Volume Glassy Polymers, Chem. Rev. 118 (2018) 5871–5911. doi:10.1021/acs.chemrev.7b00629.

[9] H.A. Mannan, H. Mukhtar, T. Murugesan, R. Nasir, D.F. Mohshim, A. Mushtaq, Recent applications of polymer blends in gas separation membranes, Chem. Eng. Technol. 36 (2013) 1838–1846. doi:10.1002/ceat.201300342.

[10] L.M. Robeson, Polymer Blends in Membrane Transport Processes, Ind. Eng. Chem. Res. 49 (2010) 11859–11865. doi:10.1021/ie100153q.

[11] R. Mahajan, W.J. Koros, Factors Controlling Successful Formation of Mixed-Matrix Gas Separation Materials, Ind. Eng. Chem. Res. 39 (2000) 2692–2696. doi:10.1021/ie990799r.

[12] S.A. Hashemifard, A.F. Ismail, T. Matsuura, A new theoretical gas permeability model using resistance modeling for mixed matrix membrane systems, J. Memb. Sci. 350 (2010) 259–268. doi:10.1016/j.memsci.2009.12.036.

[13] B. Shimekit, H. Mukhtar, T. Murugesan, Prediction of the relative permeability of gases in mixed matrix membranes, J. Memb. Sci. 373 (2011) 152–159. doi:10.1016/j.memsci.2011.02.038.

[14] T.-S. Chung, L.Y. Jiang, Y. Li, S. Kulprathipanja, Mixed matrix membranes (MMMs) comprising organic polymers with dispersed inorganic fillers for gas separation, Prog. Polym. Sci. 32 (2007) 483–507. doi:10.1016/j.progpolymsci.2007.01.008.

[15] T.T. Moore, W.J. Koros, Non-ideal effects in organic-inorganic materials for gas separation membranes, J. Mol. Struct. 739 (2005) 87–98. doi:10.1016/j.molstruc.2004.05.043.

[16] C. Ma, J.J. Urban, Polymers of Intrinsic Microporosity (PIMs) Gas Separation Membranes: A mini Review, Proc. Nat. Res. Soc. 2 (2018) 02002. doi:10.11605/j.pnrs.201802002.

[17] W.F. Yong, F.Y. Li, Y.C. Xiao, P. Li, K.P. Pramoda, Y.W. Tong, T.S. Chung, Molecular engineering of PIM-1/Matrimid blend membranes for gas separation, J. Memb. Sci. 407–408 (2012) 47–57. doi:10.1016/j.memsci.2012.03.038.

[18] W.F. Yong, F.Y. Li, Y.C. Xiao, T.S. Chung, Y.W. Tong, High performance PIM-1/Matrimid hollow fiber membranes for CO2/CH4, O2/N2 and CO2/N2 separation, J. Memb. Sci. 443 (2013) 156–169. doi:10.1016/j.memsci.2013.04.037.

[19] M.L. Jue, V. Breedveld, R.P. Lively, Defect-free PIM-1 hollow fiber membranes, J. Memb. Sci. 530 (2017) 33–41. doi:10.1016/j.memsci.2017.02.012.

[20] E. Esposito, I. Mazzei, M. Monteleone, A. Fuoco, M. Carta, N. McKeown, R. Malpass-Evans, J.C. Jansen, Highly Permeable Matrimid®/PIM-EA(H2)-TB Blend Membrane for Gas Separation, Polymers (Basel). 11 (2019) 46. doi:10.3390/polym11010046.

[21] R. Swaidan, B.S. Ghanem, E. Litwiller, I. Pinnau, Pure- and mixed-gas CO2/CH4 separation properties of PIM-1 and an amidoxime-functionalized PIM-1, J. Memb.

Sci. 457 (2014) 95–102. doi:10.1016/j.memsci.2014.01.055.

[22] P.M. Budd, E.S. Elabas, B.S. Ghanem, S. Makhseed, N.B. McKeown, K.J. Msayib, C.E. Tattershall, D. Wang, Solution-Processed, Organophilic Membrane Derived from a Polymer of Intrinsic Microporosity, Adv. Mater. 16 (2004) 456–459. doi:10.1002/adma.200306053.

[23] H.A. Patel, C.T. Yavuz, Noninvasive functionalization of polymers of intrinsic microporosity for enhanced CO2 capture, Chem. Commun. 48 (2012) 9989–9991. doi:10.1039/C2CC35392J.

[24] D. Nikolaeva, I. Azcune, E. Sheridan, M. Sandru, A. Genua, M. Tanczyk, M. Jaschik, K. Warmuzinski, J.C. Jansen, I.F.J. Vankelecom, Poly(vinylbenzyl chloride)-based poly(ionic liquids) as membranes for CO2 capture from flue gas, J. Mater. Chem. A. 5 (2017) 19808–19818. doi:10.1039/C7TA05171A.

[25] S.C. Fraga, M. Monteleone, M. Lanč, E. Esposito, A. Fuoco, L. Giorno, K. Pilnáček, K. Friess, M. Carta, N.B. McKeown, P. Izák, Z. Petrusová, J.G. Crespo, C. Brazinha, J.C. Jansen, A novel time lag method for the analysis of mixed gas diffusion in polymeric membranes by on-line mass spectrometry: Method development and validation, J. Memb. Sci. 561 (2018) 39–58. doi:10.1016/j.memsci.2018.04.029.

[26] S.S. Madaeni, M.M.S. Badieh, V. Vatanpour, Effect of coating method on gas separation by PDMS/PES membrane, Polym. Eng. Sci. (2013). doi:10.1002/pen.23456.

[27] B. Haider, M.R. Dilshad, M. Atiq Ur Rehman, J.V. Schmitz, M. Kaspereit, Highly permeable novel PDMS coated asymmetric polyethersulfone membranes loaded with SAPO-34 zeolite for carbon dioxide separation, Sep. Purif. Technol. 248 (2020) 116899. doi:10.1016/j.seppur.2020.116899.

[28] M.S. Suleman, K.K. Lau, Y.F. Yeong, Characterization and Performance Evaluation of PDMS/PSF Membrane for CO2/CH4 Separation under the Effect of Swelling, Procedia Eng. 148 (2016) 176–183. doi:10.1016/j.proeng.2016.06.525.

[29] J.M.S. Henis, M.K. Tripodi, Composite hollow fiber membranes for gas separation: the resistance model approach, J. Memb. Sci. 8 (1981) 233–246. doi:10.1016/S0376-7388(00)82312-1.

[30] A. Fuoco, C. Rizzuto, E. Tocci, M. Monteleone, E. Esposito, P.M. Budd, M. Carta, B. Comesaña-Gándara, N.B. McKeown, J.C. Jansen, The origin of size-selective gas transport through polymers of intrinsic microporosity, J. Mater. Chem. A. 7 (2019) 20121–20126. doi:10.1039/C9TA07159H.

[31] S. Keskin, S.A. Alsoy Altinkaya, A Review on Computational Modeling Tools for MOF-Based Mixed Matrix Membranes, Computation. 7 (2019) 36. doi:10.3390/computation7030036.

[32] I.N. Beckman, V.V. Teplyakov, Selective gas transfer through binary polymeric systems based on block-copolymers, Adv. Colloid Interface Sci. 222 (2015) 70–78. doi:10.1016/j.cis.2014.10.004.

[33] F. Weigelt, P. Georgopanos, S. Shishatskiy, V. Filiz, T. Brinkmann, V. Abetz, Development and Characterization of Defect-Free Matrimid® Mixed-Matrix Membranes Containing Activated Carbon Particles for Gas Separation, Polymers (Basel). 10 (2018) 51. doi:10.3390/polym10010051.

[34] S. Yi, B. Ghanem, Y. Liu, I. Pinnau, W.J. Koros, Ultraselective glassy polymer membranes with unprecedented performance for energy-efficient sour gas separation, Sci. Adv. 5 (2019) eaaw5459. doi:10.1126/sciadv.aaw5459.

[35] P. Bernardo, F. Bazzarelli, F. Tasselli, G. Clarizia, C.R. Mason, L. Maynard-Atem, P.M. Budd, M. Lanč, K. Pilnáček, O. Vopička, K. Friess, D. Fritsch, Y.P. Yampolskii, V. Shantarovich, J.C. Jansen, Effect of physical aging on the gas transport and sorption in PIM-1 membranes, Polymer (Guildf). 113 (2017) 283–294. doi:10.1016/j.polymer.2016.10.040.